Flow and pressure field measurement of turbulent round jet impinging on a circular cylinder

Mirae Kim[1], Yongzeng Li[2], Eunseop Yeom[1], Kyung Chun Kim[1]*

[1] Pusan National University, School of Mechanical Engineering, Busan, Republic of Korea

[2] Shanghai Jiao Tong University, School of Mechanical Engineering, Shanghai, China

*corresponding.kckim@pusan.ac.kr

Abstract

Flow characteristics in a round jet impingement onto a circular cylinder with 45 degrees inclination angle were visualized by particle image velocimetry (PIV) measurements. Reynolds number based on the round jet volumetric flow is 11800. In order to verify the PIV results, surface pressure measurements using pressure sensitive paint (PSP) and large eddy simulation (LES) were made at the same flow condition. After impingement, the jet becomes a 3D curved wall jet and being attached far downstream to the cylinder wall due to the Coanda effect. At a same impinging angle, flow separation is delayed with increasing Reynolds number. A self-preserving phenomenon of wall jet profile was not clearly appeared in the 3D curved wall jet. Turbulent characteristics were by turbulence intensity and the Reynolds shear stress. The Reynolds shear stress decreases downstream of the cylinder wall due to the decreased velocity and centrifugal force. Time averaged pressure field confirms that the jet attachment is caused by the strong suction pressure after impingement. The PSP results also showed the same tendency of flow separation as the PIV results. The ensemble-averaged velocity fields show good agreement between PIV and LES results.

1 Introduction

Jet impingement has long been used as a direct and efficient way to transfer heat and is encountered in numerous applications. Many applications involve flows impinging on surfaces that are not flat. Compare to a plane turbulent wall jet, there are many interesting phenomena such as the Coanda effect, curvature of wall jet boundary layer, and flow separation (Azim (2013), Danon et al. (2016)). Also the flow field presents unique flow geometry where an axisymmetric jet becomes a three-dimensional flow over the surface. However, less attention has been given to circular jet impingements on other types of surface geometries, particularly curved surfaces. Even if there is a study of a single round jet impinging on a cylindrical convex surface, the studies have limitations such as smoke wire visualization (Cornaro et al. (1999)), laminar flow (New and Long (2015)), and small details on a latter flow mechanism Esirgemez et al. (2007). Mean and turbulent flow characteristics of the 3D curved wall jet on a cylinder measured by 2D PIV were reported in our previous paper (Kim et al (2018)). The present study sheds more light on the flow separation of the 3D curved wall jet on a convex circular cylinder. This was accomplished using a pressure sensitive paint and large eddy simulation measurements.

2 Methods

Fig. 1 (a) shows a schematic of the flow configuration and the coordinate system of the curved wall jet. The whole field of view for the PIV measurement included the curved wall jet area over half of the cylinder in the wall normal direction, including the impinging area. Due to the limitations of the fields of

view, different fields of view were reconstructed by merging two subsections except the impinging area. For each section, PIV parameters, such as time interval were different to optimize the PIV measurement. Impinging angle (α) was defined the angle between jet axis to normal direction of the circular cylinder. Reynolds number was defined as $(4Q/\pi d^2)\cdot d/\nu$, where Q is the jet volumetric flow rate and d is the nozzle diameter. Three different Reynolds numbers and four different nozzle angles were selected as parameters. An Nd:Yag pulse laser was used for illumination and a CCD camera was used to obtain particle image. Velocity vectors were obtained using a two-frame cross-correlation method and a post-processing program (PIVACE) was used to remove error vectors and corrected vectors were replaced by an interpolation method. 1000 PIV realizations were used to obtain ensemble averaged velocity field.
Surface pressure measurement was performed using fast-responding pressure-sensitive paint (fast PSP). Fast PSP is an optical technique suitable for measurement of time resolved surface pressure distributions on the order of kilohertz. The schematic of PSP measurement setup is shown in Fig. 1 (b). The PSP is comprised of an oxygen sensitive luminophore and a binder, with the luminophore emitting luminescence when excited by light and the binder holding the luminophore onto the tested object. For the purposes of surface pressure visualization, pure nitrogen was blown though the nozzle instead of air. A UV LED was used to excite the luminophore, and a high speed camera with CMOS 800 × 600 sensor was used to capture the emitted luminescence. The images were acquired at a frame rate of 2000 Hz.
LES also conducted by same flow configuration and coordinate system in Fig. 1 (a). The Navier-Stokes equations were discretized by the finite-volume method (FVM). A computational domain with a structured mesh was designed with 1.8×10^6 cells. To increase the quality of the simulations, a boundary layer mesh was established around the wall surface of the cylinder. No-slip conditions are applied to the wall surface of the cylinder, and the outer boundaries have outlet conditions with atmospheric pressure. The jet velocity in the nozzle is set as an inlet velocity with uniform flow. The turbulence intensity measured by PIV at the inlet of the nozzle, 22% was added to the inlet velocity to have the same conditions as the experimental case. The results showed that errors of 10.08% and 0.13% were obtained for the respective velocity profile deviations resulting from coarse and fine meshes compared to the very fine mesh. Therefore, the fine mesh was used for the rest of the investigations.

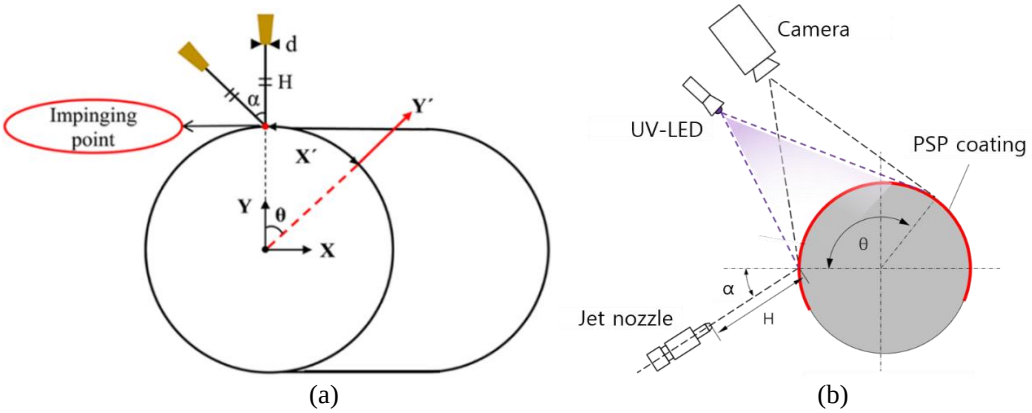

Figure 1: (a) Flow configuration and (b) schematic of pressure measurement system.

3 Results and Discussion

The whole velocity field and the surface pressure field of the impinging jet onto a cylinder is shown in Fig. 2. The 3D curved wall jet develops along the curved surface after the impingement. When the impinging angle is 45°, most of the impinged jet fluid moves in the clockwise direction. Compared to normal impingement, the oblique impinging jet produces higher momentum and thickness of the curved wall jet. For both cases, the wall jet is attached to the cylinder wall due to the Coanda effect, even though

the velocity continuously decreases. The separation point occurs at a cylinder angle of about 125° at the lowest Reynolds number. The separation points are further downstream compared to those observed with uniform laminar flow over a cylinder. The flow separation occurs around 170° to 180° from the impinging point in the longitudinal direction at the highest Reynolds number. Pressure fields for both impinging angles show strong suction pressure after impingement. At high impinging angle, the elongated suction pressure region on the cylinder reveals the delayed separation due to lower adverse pressure gradient.

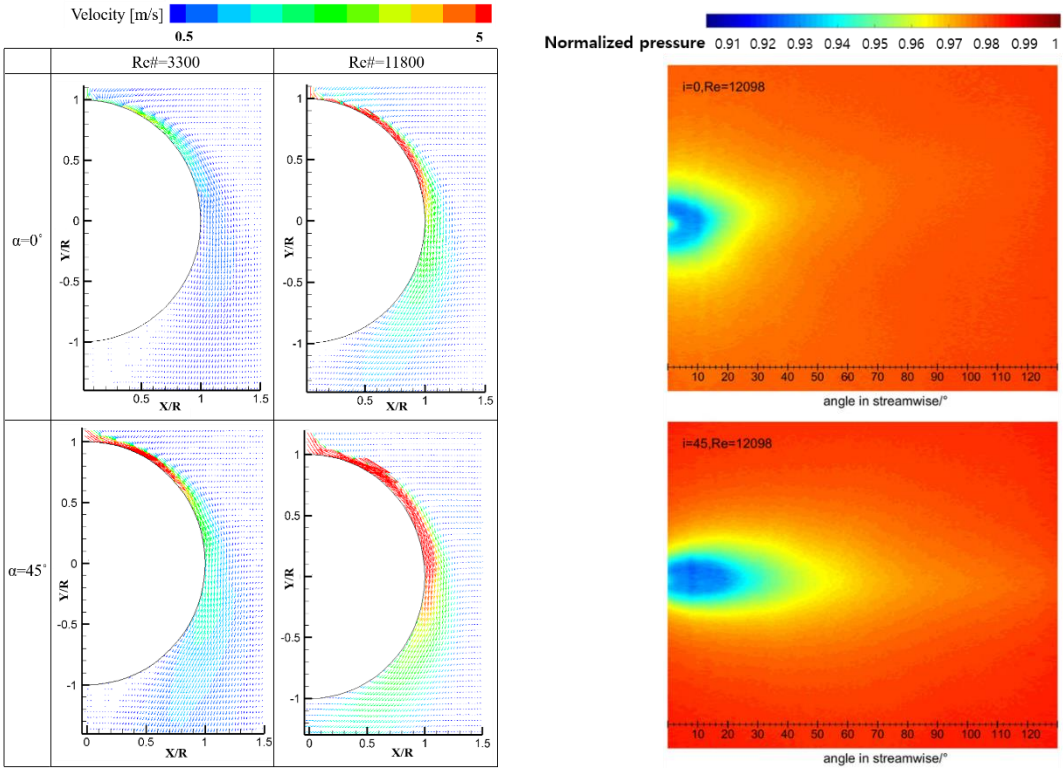

Figure 2: Velocity and surface pressure fields over the circular cylinder after a round jet impinges onto a cylinder with respect to various Reynolds number and impinging angle.

Fig. 3 (a) shows the time-averaged velocity contours from when the flow reaches steady state conditions. After the 45° oblique impingement of a round jet onto the cylinder surface, most of the fluid moves in one direction. At a Reynolds number of 11800, the round jet impinges with a speed of 60 m/s and then quickly slows down further downstream. There is good agreement between the whole velocity fields obtained by LES and PIV, as shown in Fig. 3 (a). The 3D curved wall jet develops along the curved surface after the impingement. Fig. 3 (b) shows comparisons of the velocity profiles obtained at three different positions (θ = 15°, 60°, and 120°). The LES results show excellent agreement with the PIV results. Fig. 3 (b) shows that self-preserving wall jet profiles did not occur because the wall jet could not fully develop due to flow separation. Significant variations of the mean velocity profiles near the wall region are observed in the flow direction. Compared to the results from a 2D curved wall jet, the maximum velocity point is higher from the wall. This can be explained by the lateral momentum flux in the case of the 3D curved wall jet, which is followed by a rapid decrease of the longitudinal momentum in the flow direction. As a result, flow separation occurs earlier than in the case of a 2D curved wall jet.

Fig. 4 (a) shows the normalized streamwise turbulence intensity profiles at various downstream positions. Compared to the mean velocity profiles, the turbulence intensity profiles do not coincide well in normal impingement case. In the case of a 2D curved wall jet from a slot jet, both the streamwise and radial turbulence intensities increase with X′/d. However, the maximum streamwise turbulence intensity

decreases as X´/d increases in the case of a 3D curved wall jet. The maximum streamwise turbulence intensity at θ =15° is 2.3 times larger than that at θ=120°. The main reason for the difference between the 2D curved wall jet and 3D curved wall jet is that the streamwise velocity magnitude decreases with X´/d due to the 3D wall jet spreading in not only the streamwise direction but also the lateral direction. In 45° oblique impingement case, the turbulence intensities are much more similar to that of a 2D curved jet. The maximum streamwise turbulence intensity increases with the development of the 3D curved wall jet as in a 2D curved wall jet until X´/d = 8.73, and then it decreases with a reduced mean velocity. In the case of impingement at 45°, the maximum streamwise turbulence intensity at θ =15° is 1.3 times larger than that at θ =120°. Fig. 4 (b) shows the contours of the normalized Reynolds shear stress distribution with streamline. The impinging angle has a strong effect on the Reynolds shear stress. When the Reynolds number is the same, positive Reynolds shear stress is distributed further along the cylinder surface as the impinging angle increases. The turbulence characteristics of the 3D curved wall jet are different compare to the plane wall jet and the 2D curved wall jet. In the case of the 3D curved wall jet, the Reynolds shear stress decreases downstream unlike a 2D curved wall jet. This is because, the rapid decrease in the streamwise mean velocity followed by a weakened centrifugal force.

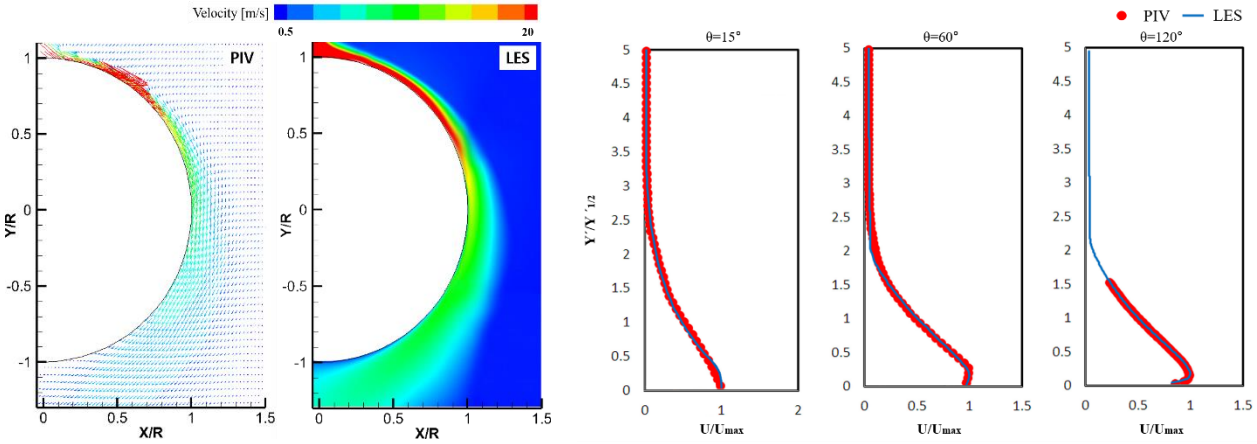

(a) (b)

Figure 3: Comparison of PIV and LES results (a) ensemble velocity contours, (b) mean velocity profiles.

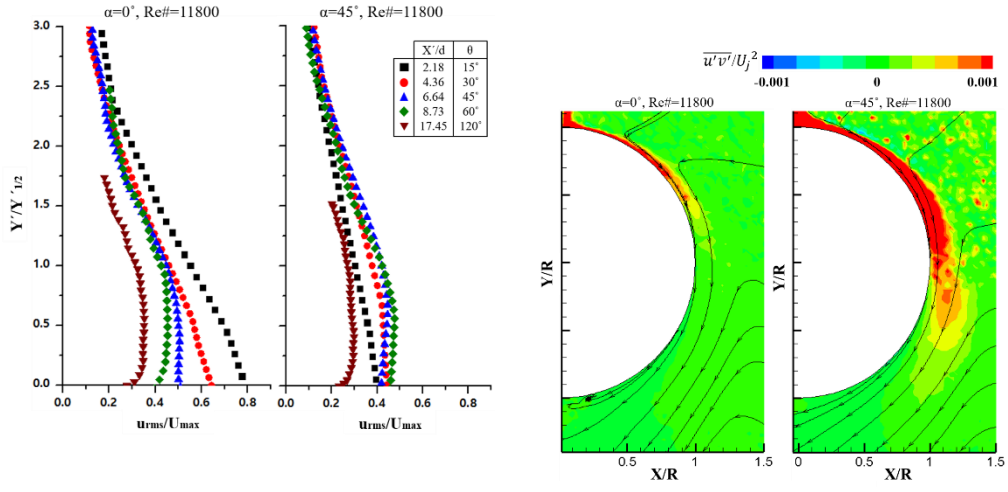

(a) (b)

Figure 4: (a) Streamwise turbulent intensity profiles, (b) Reynolds shear stress contours.

Conclusion

The flow and pressure field of oblique jets impinging onto a circular cylinder were analyzed by conventional PIV, fast PSP and LES measurements. Different fields of view were adopted to capture the different velocity magnitudes in impinging area and 3D curved wall jet progression part. The separation point occurs later when the higher impinging angle and Reynolds number. At the highest Reynolds number except under normal impingement, the flow attaches at almost halfway around the cylinder in the longitudinal direction due to the Coanda effect. The self-preserving wall jet profile was not attained in the 3D curved wall jet. At the same Reynolds number, the initial momentum of the wall jet is increased when the impinging angle increases therefore, most of the flow follows in one direction and the momentum is higher compare with lower impinging angle. In contrast to the 2D curved wall jet, the streamwise turbulence intensity decreases with increasing streamwise distance. The Reynolds shear stress normalized by the jet exit velocity is more affected by the impinging angle than the Reynolds number. Fast PSP measurement results show that, due to the adverse pressure gradient reduces as impinging angle increases the separating tendency delays. By comparing the time-averaged velocity contours and profiles, we can see that the 2D PIV results are in good agreement with the 3D LES results.

Acknowledgements

This study was supported by the National Research Foundation of Korea (NRF) grant funded by the Korean government (MSIT) (No. 2018R1A2B2007117).

References

Azim MA (2013) On the Structure of a Plane Turbulent Wall Jet. *Journal of Fluids Engineering* 135: 084502.

Danon R, Gregory JW and D. Greenblatt D (2016) Transient wall jet flowing over a circular cylinder. *Experiments in Fluids* 57: 1-14.

Cornaro JC, Fleischer AS and Goldstein RJ (1999) Flow visualization of a round jet impinging on cylindrical surfaces. *Experimental Thermal and Fluid Science* 20: 66-78.

New TH, Long J (2015) Dynamics of laminar circular jet impingement on convex cylinders, P*hysics of Fluids* 27: 024109.

Esirgemez E, Newby JW, Nott C, Ölçmen SM and Ötügen V (2007) Experimental study of a round jet impinging on a convex cylinder. *Measurement Science and Technology* 18: 1800-1810.

Kim M, Kim HD, Yeom E and Kim KC (2018) Flow characteristics of three-dimensional curved wall jets on a cylinder. *ASME Journal of Fluids Engineering* 140: 041201.